

Circular, Plane-Directional Radiation from the Edges of Light-Excited Layer of a Laser Dye Solution with the Regular Geometric Form

Zurab V Wardosanidze^{1,2*}

¹*Institute of Cybernetics of the Georgian Technical University, Georgia*

²*LEPL Ilia Vekua Sukhumi Institute of Physics and Technology, Georgia*

Abstract

Homogeneous light excitation of the Rhodamine 6G laser dye alcohol solution layer of rectangular and circular geometric form by the second harmonic of Nd:YAG (532 nm) laser is realized. A circular, plane-directed radiation from the edges of the excited layer with a small, vertical, divergence was obtained. Was investigated experimentally the spectral and spatial characteristics of radiation. The investigated layer is a part of the dye solution that is in direct contact with the bottom of the optical cells, the rectangular and circular sections of which determine geometric shape of the layer. Excitation of the layer was performed from the side of the cell bottom. It turned out that within the concentrations of the dye in the solution from 0.12w% to 0.03w%, the following processes are observed: Planely directed uniform, in intensity, radiation around the cell in the plane of the luminescent layer with a small vertical divergence; An increase in the amplitude of radiation pulses with a decrease in the concentration of the dye in the solution from 0.12w% to 0.03w%; Shifting of the maximum of the emission spectrum to the short-wave region, significant narrowing of the radiation spectrum and decrease of the vertical divergence of radiation.

Keywords

Light-excitation, Superluminescence, Superradiance, Spectrum, Coherence, Total internal reflection

Introduction

The investigated layer in combination with an optical cell can be considered as a monolithic ring resonator (MRR), operating on the basis of total internal reflection (TIR) [1,2]. In this case, the main directions of maximal Q-factor (lasing) inside of cells, must satisfy the condition of total internal reflection (TIR): $\alpha = \beta \geq \arcsin \frac{n_1}{n_2}$, where $\alpha =$

β are the angles of incidence and reflection, n_2 is the refractive index of the optical cell wall, n_1 is the refractive index of air.

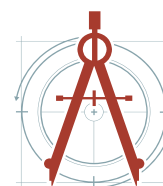
For the rectangular cell, the main directions coincide with the sides of the inscribed rectangles parallel to the diagonals, which can ensure lasing, practically, in the entire dye layer (Figure 1a). For the cylindrical cell, the main directions form a kind of corona at the periphery will creating conditions for the lasing far from the center, near the walls

***Corresponding author:** Zurab V Wardosanidze, Institute of Cybernetics of the Georgian Technical University 5, ZurabAndjaparidze Str., 0186 Tbilisi, Georgia; LEPL Ilia Vekua Sukhumi Institute of Physics and Technology, 7, Mindeli Str., 0186 Tbilisi, Georgia

Accepted: November 20, 2021; Published: November 22, 2021

Copyright: © 2021 Wardosanidze ZV. This is an open-access article distributed under the terms of the Creative Commons Attribution License, which permits unrestricted use, distribution, and reproduction in any medium, provided the original author and source are credited.

Wardosanidze. Int J Opt Photonic Eng 2021, 6:041



Citation: Wardosanidze ZV (2021) Circular, Plane-Directional Radiation from the Edges of Light-Excited Layer of a Laser Dye Solution with the Regular Geometric Form. Int J Opt Photonic Eng 6:041

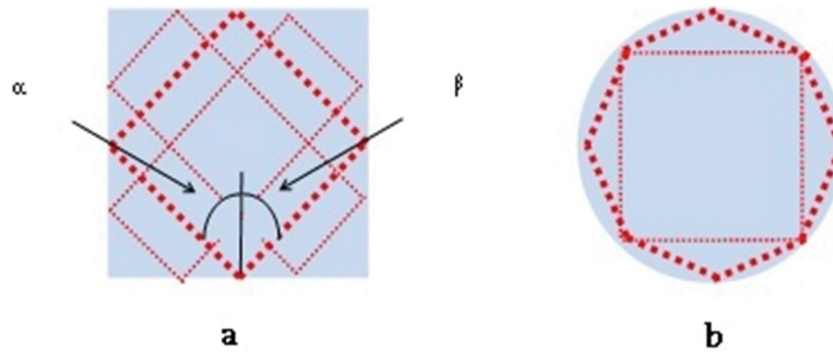


Figure 1: Main directions of intracavity lasing (MRR - TIR) for rectangular (a) and cylindrical (b) cells.

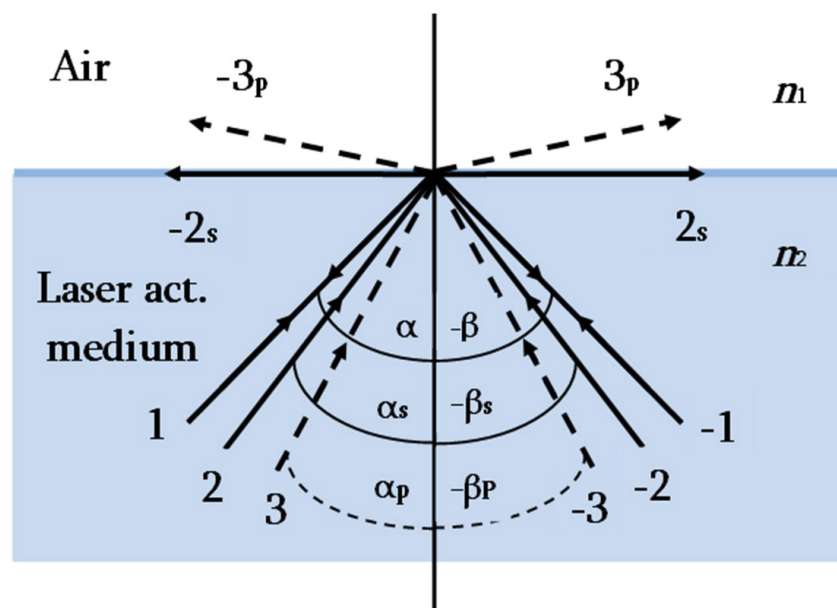


Figure 2: The scheme of propagation of the beams in the MRR near to the angle of TIR.

1, -1 - beams directions at angles $(\alpha, -\beta)$ of TIR; 2, -2_s - beams directions at critical angles $(\alpha_s, -\beta_s)$; 3, -3 - beams directions at a little less of critical angle $(\alpha_p, -\beta_p)$; 2_s, -2_s - sliding beams of light when the critical angle; 3_p, -3_p - penetrating through the interface light beams when an angle of incidence is less than critical.

of the cell (Figure 1b) [2]. Total internal reflection (TIR) from the cell walls will provide lasing within the cells only, that will be enclosed in a layer of dye solution and cannot leave the optical cell. To output the generated light from such a resonator, it is necessary to violate the condition of total internal reflection at some point of the cell walls in the plane of the emitted layer [1,2].

However, in addition to the main directions, the population inversion created in the layer should provide amplification of radiation in other directions that are not subject to total internal reflection. It's obvious that, these radiations already can leave the optical cell (resonator) in the form of Superradiance, Superluminescence and, may be, lasing in the resonator, formed as a result of

Fresnel reflection, for normal incidence of beams, on the walls of the cell [3-12].

The path of rays with angles of incidence less than the critical angle of total internal reflection deserves special attention. In particular, for the ring resonators shown in Figure 1, beams with incidence angles slightly

less than the critical angle of total internal reflection

(TIR) $\alpha = \beta \leq \arcsin \frac{n_1}{n_2}$ must leave the resonator

(Figure 2). Here 1, -1 are paths of beams inside of MRR at total internal reflection at angles $\alpha = -\beta$; 2, -2 and 2_s, -2_s - are paths of beams at critical angle of total internal reflection ($\alpha_s = -\beta_s$); and 3, -3 and 3_p, -3_p are paths of beams less of critical angle of total internal

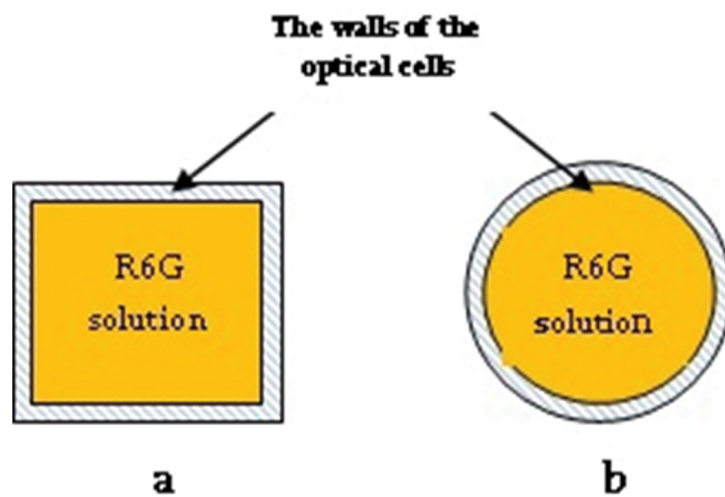


Figure 3: Schematic images of the cross-section of rectangular (a) and cylindrical (b) cells filled with a dye solution.

reflection ($\alpha_p = -\theta_p$). In this case $2_s, -2_s$ - are paths of sliding beams along the interface at the critical angle of incidence and $3_p, -3_p$ - are penetrating beams through the interface light when an angle of incidence is less than critical. Here it is taken into account that beams are falling on the interface of MRR-Air from both sides symmetrically to the normal to the surface. On the other hand, it should be borne in mind that at angles less than the angle of total internal reflection, some of the beams are, nevertheless, reflected inside the resonator, the intensity of which depends on the reflection coefficient from the interface MRR-Air. Q-factor of MRR in this case is determined, mostly, by refractive index of the walls of the optical cells and of incidence angles of the light calculation of which is separate research problem. A small difference in the refractive indices ($\Delta \approx 0.14$) of the dye solution and the walls of the optical cell practically does not affect the main process. Accordingly, for some directions of internal beams near to TIR angle there exist a possibility ring resonators can have a certain Q-factor sufficient for lasing which may be radiated from MRR. For a ring resonator with a cross-section in the form of a rectangle or a circle, this condition should be satisfied much efficiently due to the wider range of the main directions of the effective Q-factor. Due to great amplification along the layer, these radiations, outside of resonator, will be more intense in the plane of excited layer and should have a uniform circular distribution around the optical cell [3-10].

Experimental Results

For observing and investigation of radiation of the dye solution layer, the experiments were carried

out with an alcohol (ethyl alcohol) solution of the laser dye Rhodamine 6G, placed in rectangular and cylindrical optical cells made of isotropic optical glass K8 with a refractive index $n'_g = 1.51$. The alcohol solutions of Rodhamine 6G (R6G) were prepared with various concentrations: 0.15(w%); 0.12(w%); 0.09(w%); 0.06(w%); 0.03(w%); with an average refraction index $n'_2 = 1.37$. The schematic images of the cross-section of rectangular and cylindrical cell filled with a dye solution and their photographic images are shown in Figure 3 and Figure 4.

Inside size of the rectangular cell is 18×20 mm and inside diameter of the cylindrical cell is 28 mm and the thickness of their glass walls is 3 mm, quite satisfying the conditions of a monolithic ring resonator (MRR). Optical excitation (pumping) was carried out by the second harmonic of aNd: YAG ($\lambda = 532$ nm), from the side of the bottom of the optical cell, at a strict perpendicularity of the luminescent layer of the dye solution to the walls of the cell and to the pumping beam. The set-up scheme is shown in Figure 5. The second harmonic of a Nd:YAG laser ($\lambda = 532$ nm) is expanded by a collimator and after the diaphragm forms a rectangular or circular light spot with a size and form corresponding to the size and profile of the cell bottoms. The total internal reflection prism, having a stable optical contact with the bottom of the optical cell, deflects the beam by 90° and directs it perpendicular to the bottom of the optical cell, i.e., to the plane of the excited layer. The energy density of the pumping light was $0.2-0.3$ J/cm² and the duration of the pulses of the

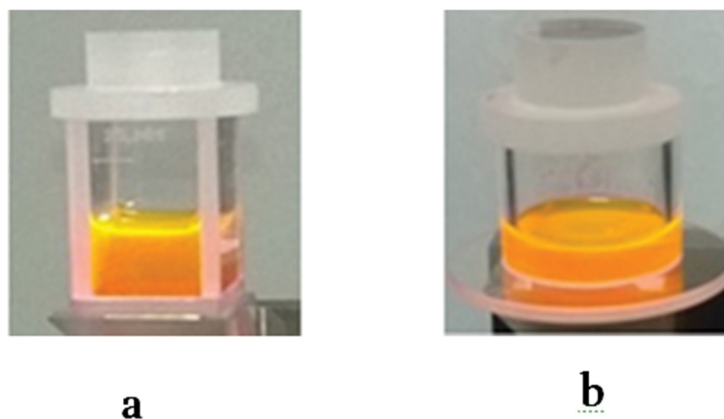


Figure 4: Photos of the rectangular (a) and cylindrical (b) cells with R6G solution.

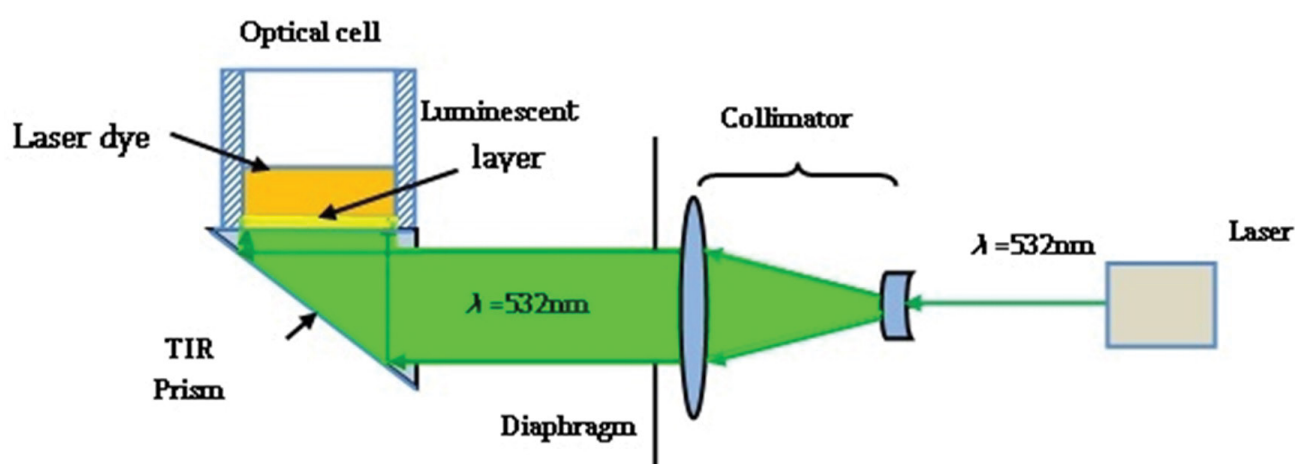


Figure 5: The optical scheme of the set-up.

pumping was $\tau \approx 10$ ns, which are sufficient to create a significant population inversion in the layer. Consequently, intense spontaneous and induced transitions should acquire an avalanche character, leading to Superradiance and Superluminescence [3-10,13-17].

The projections of radiation onto a round and flat screen of the excited layer formed by a rectangular cell is shown in Figure 6a and Figure 6b, respectively. Figure 6 clearly shows the uniform distribution of the radiation intensity in the plane of the excited layer around the optical cell.

Was investigated the spectral characteristics of radiation in the different dye concentrations in solution. It turned out that with a decrease in the concentration of the dye from 0.12w% up to 0.03w%, the peak energy of the radiation pulses increases and reaches the saturation value (Figure 7).

The spectral curves of the radiation of the excited

layer of the solution were obtained at identical pump radiation energy ($\lambda = 532$ nm). According to Figure 7, with a decrease in the concentration of the dye from 0.12wt% to 0.06wt%, the radiation energy increases from the very beginning, and at a minimum concentration of 0.03wt% it already decreases, which is probably associated with concentration effects (concentration quenching, quantum yield). At the same time, with a decrease in the concentration of the dye, the radiation spectrum narrows and already at a concentration of 0.03 (w%), the half-width of the radiation spectrum reaches 3-4 nm, which is typical for Superradiance, Superluminescence, and even for lasing (Figure 7 - Figure 4). A further decrease in the concentration of the dye leads to a significant decrease in the intensity of radiation and to a broadening of the emission spectrum up to usual luminescence Figure 8.

Similar experiments were carried out for a cylindrical optical cell in the same conditions of the

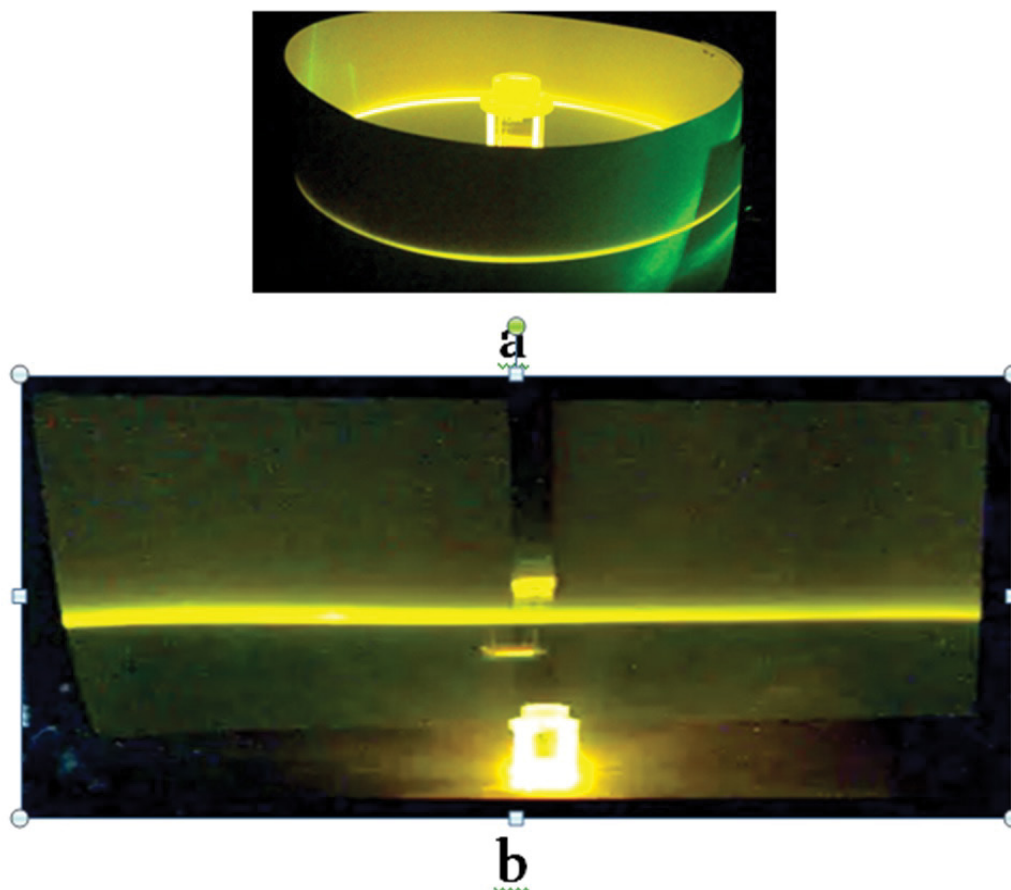


Figure 6: Light emission from an excited layer of an alcohol solution of the dye Rhodamine 6G bordered by the rectangular optical cell.

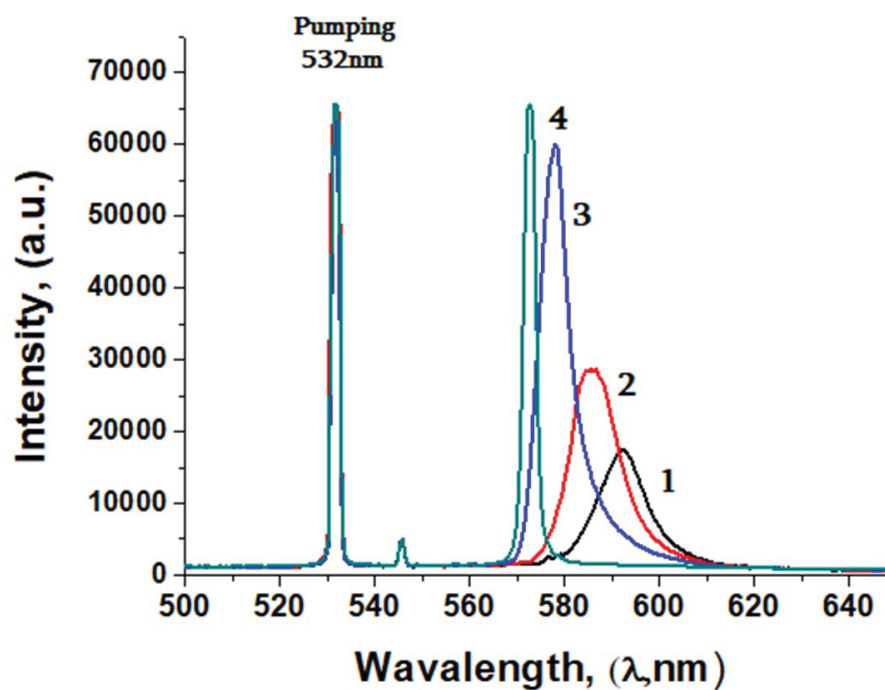


Figure 7: The spectrums of emission of the excited layer for the different concentrations of the dye (1 - 0.12w%; 2 - 0.09w%; 3-0.06w%; 4 - 0.03w%) for the rectangle cell.

pumping and the same concentrations of the dye R6G. The character of emission of excited layer in the cylindrical cell is almost identical to emission of

in the rectangular cell (Figure 6; Figure 9).

Figure 9a and Figure 9b displays the projections of emission of a cylindrical cell on the round and

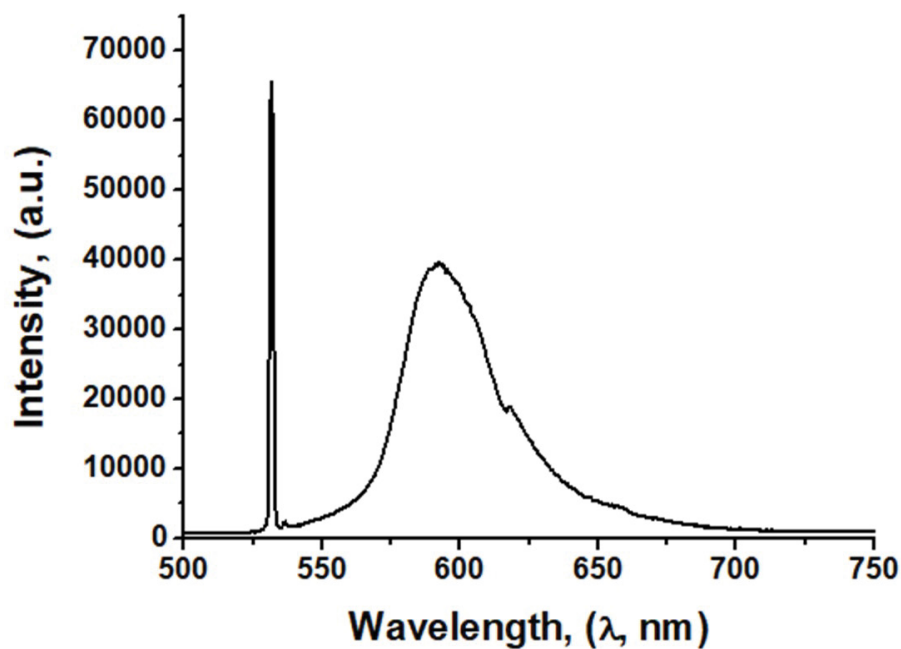
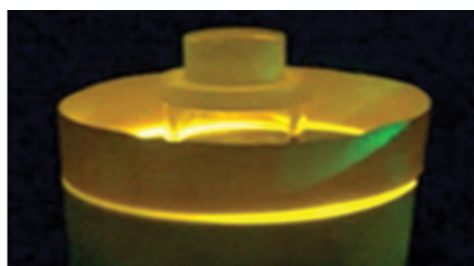


Figure 8: Usual fluorescence of the layer of R6G solution at the concentration 0.007w%.



a



b

Figure 9: Light emission from an excited layer of an alcoholic solution of the dye Rhodamine 6G bordered by the cylindrical optical cell.

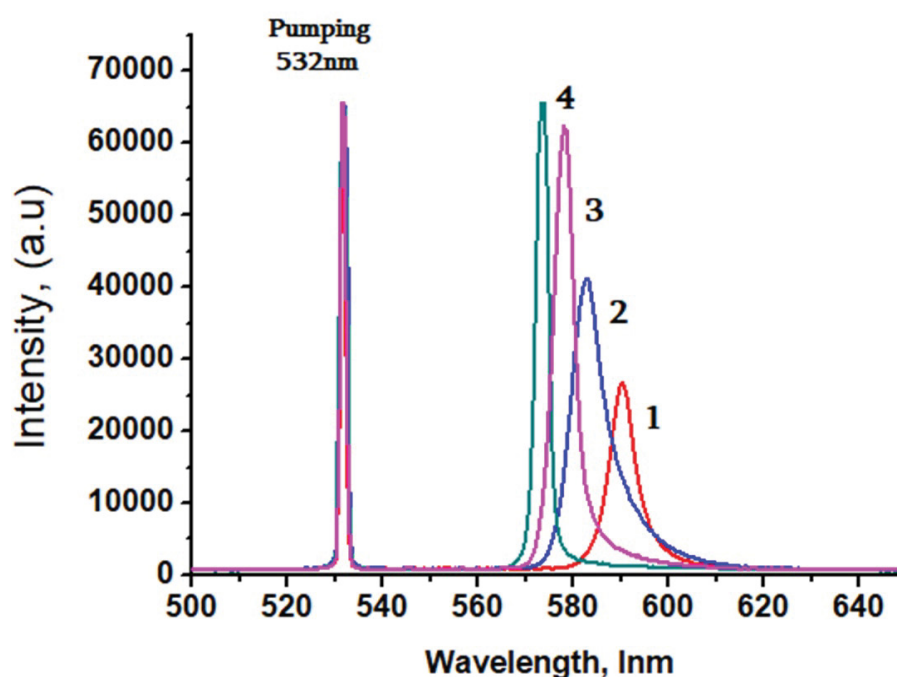


Figure 10: The spectrums of light emission of the dye solution layer at the different concentrations of the dye (1 - 0.12w%; 2 - 0.09w%; 3-0.06w%; 4 - 0.03w%) for the cylindrical cell.

flat screens, respectively that confirm the uniform distribution of radiation around the cell in the plane of the excited layer.

The spectral characteristics of the radiation of the layer of the solution of R6G, for a cylindrical cell, at different concentrations of the dye (1 - 0.12w%; 2 - 0.09w%; 3-0.06w%; 4 - 0.03w%) in an alcohol solution are shown in Figure 10. As expected, in this case, too, with a decrease in the concentration of the dye, the emission spectrum narrows and at a concentration of 0.03 (w%) approaches the spectrum characteristic of Superradiance, Superluminescence, and lasing (3-4 nm). At the same time the spectrum maximum of radiation shifts to the short wavelength area and peak of emission energy increases up to saturation. The nature of the dependence of the energy efficiency on the concentration is practically the same as for a rectangular cell. The rest, everything, is repeated, in approximately the same way as in the case of a rectangular optical cell.

As it was noted above, with a decrease in the concentration of the dye, in addition to the shifting of the spectrum of maximums and narrowing of the emission spectrum, the vertical divergence of radiation for both cells also decreases. Figure 11 is showing projections of the radiation, of excited

layer in rectangle (a) and cylindrical (b) cell, on a flat screen, at the dye concentrations: 0.12w%; 0.09w%; 0.06w% and 0.03w% which illustrate decreasing of vertical divergence of the emitted light.

The dependence of the vertical divergence of radiation of the dye concentration is represented in Figure 12. Figure 12a, corresponds to emission vertical divergence for the rectangle cell and Figure 12b corresponds to vertical divergence of light emission for the cylindrical cell.

According to Figure 12 initial, vertical, divergence of the emitted light from the rectangle cell at dye concentration 0.12w% is great (about 10 mrad) than the divergence for the cylindrical cell (7.6 mrad) in the same concentration of the dye. At the dye concentration 0.09w% the vertical divergence of radiation of both optical cells are identical. With a further decrease in the concentration of the dye, the vertical divergence of the radiation decreases faster for a rectangular cell than for a cylindrical cell and reaches 2.5-3 mrad. These results need additional separate investigation that will be realized in the nearest future.

The study of spatial coherence showed its practical absence. With regard to temporal coherence, the radiation provided fairly clear

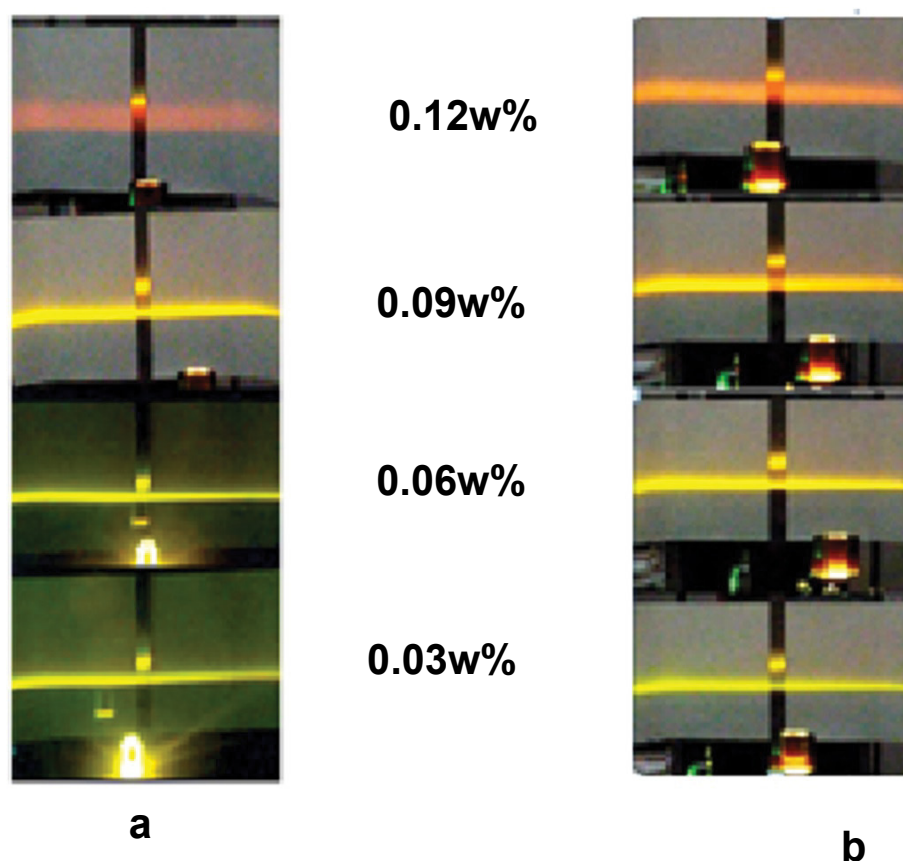


Figure 11: Projections of emission of excited layer in the rectangle (a) and cylindrical (b) cells on a flat screen for different concentrations (1 - 0.12w%; 2 - 0.09w%; 3-0.06w%; 4 - 0.03w%) of dye R6G.

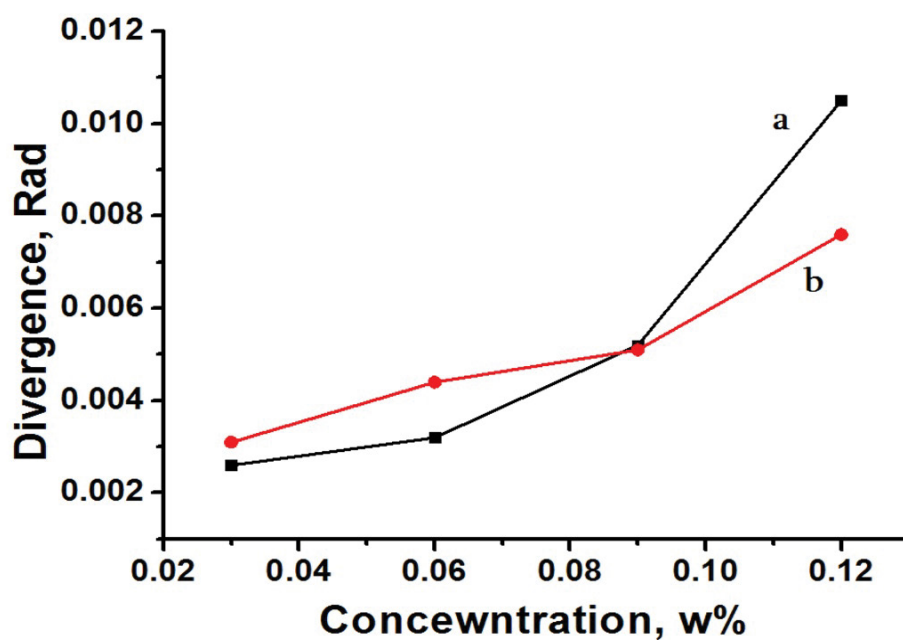


Figure 12: The dependence of vertical divergence of emission of excited layer in the rectangle (a) and cylindrical (b) cells.

interference when dividing the amplitude with a path difference of 1.0 cm for beams with a diameter of 0.5 mm, cut off by the corresponding diaphragm and subsequently divided into two identical beams. Emitted light is unpolarized.

Discussion

So, was obtained narrowband (3-14 nm) radiation of the thin layer, of rectangle and circular geometrical form, of the laser dye R6G solution. This radiation is characterized with uniform circular distribution of emitted light in the layer plane with sufficient low vertical divergence (2-10 mrad).

As is known, with a change in the dye concentration, the penetration depth of pump radiation into the dye solution (in the case of linear absorption) changes according to the law [11,12]:

$$d = \frac{\ln I_0 - \ln I_{act}}{k_\lambda}$$

Where I_0 is the intensity of the incident pump light, I_{act} is the intensity of the penetrated pump light in the absorbing solution of the dye which is sufficient for the population inversion, and k_λ is the absorption coefficient at the pump wavelength $\lambda = 532$ nm. It should be noted that accurate measurement of an active luminescent layer subjected to population inversion is a rather difficult task and it needs a separate study, which also is planned for the future. According to approximate measurements with an adjustable diaphragm, the thickness of the active super radiant and super luminescent parts of the excited layer varies in the range of 40-250 μ m.

The almost complete absence of spatial coherence and low temporal coherence indicates a lack of radiation as a result of the lasing. This also indicates that the conditions for super radiant lasing according to Dicke and super luminescent lasing in one pass were not achieved, which indicates insufficient excitation of the luminescent layer to achieve a maximal population inversion [3-17].

Conclusion

For seepage outward, behind the walls of the cell, the angle of incidence of the beams from the side of the dye solution layer at the optical cell glass-air interface must be low of the critical angle of the TIR and must satisfy the condition $\alpha = \beta \leq \arcsin \frac{n_g}{n}$ i.e., $\alpha = \beta \leq 45^\circ$. It is naturally that light beams incident at smaller angles also pass through the glass

walls of the cell, moreover, with less losses. Thus, with an increase in the density of the excitation (pumping) energy, it is possible to achieve greater coherence of radiation in the achieving the Dicke condition and obtain radiation with better spectral characteristics and obtain the laser radiation [3]. In the author's opinion, it is of some interest to continue the study at higher pump intensity densities, which may reveal new characteristics of the radiation of the device model presented in this work. From the point of view of the applied optics, the results obtained can be used to create a laser beacon, the efficiency of which will be much better than the existing, at this time, similar devices.

Certain differences between the radiation of the luminescent layer of an excited dye of rectangular and circular geometric shapes require additional study that already is on the stage of investigation.

References

- Schiller S, Fejer MM, Byer RL, Sizmann A, Karim M (1992) Monolithic total internal reflection resonators: Principles and applications. Conference on Lasers and Electro-Optics, Anaheim, California, United States, 10-15.
- Lina G, Chembo YK (2019) Monolithic total internal reflection resonators for applications in photonics. Optical Materials X 2: 100017.
- Dicke Robert H (1954) Coherence in spontaneous radiation processes. Physical Review 93: 99-110.
- Gross M, Haroche S (1982) Superradiance: An essay on the theory of collective spontaneous emission. Physics Reports 93: 301-396.
- Bekenstein JD, Schiffer M (1998) The many faces of Superradiance. Physical Review D 58: 1-13.
- Rehler NE, Eberly JH (1971) Superradiance. Phys Rev A 3: 1735-1751.
- Scully MO, Svidzinsky AA (2009) The super of Superradiance. Science 325: 1510-1511.
- Barnes NP, Walsh BM (1999) Amplified spontaneous emission - application to Nd:YAG lasers. IEEE J Quantum Electron 35: 101-109.
- Blazek M, Hartmann S, Molitor A, Elsaesser W (2011) Unifying intensity noise and second-order coherence properties of amplified spontaneous emission sources. Opt Lett 36: 3455-3457.
- Keppler S, Savert A, Korner J, Hornung M, Liebetrau H, et al. (2016) The generation of amplified spontaneous emission in high-power CPA laser

- systems. Laser Photon Rev 10: 264-277.
11. Born M, Wolf E (1964) Principles of optics. (2nd edn), Pergamon Press, UK, 936.
 12. Wood RW (1988) Physical optics. (3rd edn), Optical Society of America, Washington, 846.
 13. Scheibner M, Schmidt T, Worschech L, Forchel A, Bacher G, et al. (2007) Superradiance of quantum dots. Nature Physics 3: 106-110.
 14. Bonnet JG, Chen Z, Weiner JM, Meiser D, Holland MJ, et al. (2012) A steady-state superradiant laser with less than one intracavity photon. Nature 484: 78-81.
 15. Weiner JM, Cox KC, Bohnet JG, Thompson JK (2017) Phase synchronization inside a superradiant laser. Phys Rev A 95: 1-5.
 16. Laske T, Winter H, Hemmerich A (2019) Pulse delay time statistics in a superradiant laser with calcium atoms. Phys Rev Lett 123: 1-5.
 17. Liu H, Jäger SB, Yu X, Touzard S, Shankar A, et al. (2020) Rugged mHz-Line width superradiant laser driven by a hot atomic beam. Phys Rev Lett 125: 1-6.

